β-Ga₂O₃ used as a saturable absorber to realize passively Q-switched laser output

Baizhong Li [1,2], Qiudi Chen [3], Peixiong Zhang [3,*], Ruifeng Tian [1,2], Lu Zhang [1,2], Qinglin Sai [1], Bin Wang [1], Mingyan Pan [1] , Youchen liu [1], Changtai Xia [1], Zhenqiang Chen [3], and Hongji Qi [1*]

[1] Key Laboratory of Materials for High Power Laser, Shanghai Institute of Optics and Fine Mechanics, Chinese Academy of Sciences, Shanghai 201800, China; lbz446@siom.ac.cn (B.L.); ruifengtian@siom.ac.cn (R.T.); zhanglu@siom.ac.cn (L.Z.); saiql@siom.ac.cn (Q.S.); wangbinmars@siom.ac.cn (B.W.); pmy@siom.ac.cn (M.P.); lyc@siom.ac.cn (Y.L.); xia_ct@siom.ac.cn (C.X.)

[2] Center of Materials Science and Optoelectronics Engineering, University of Chinese Academy of Sciences, Beijing, 100049, China

[3] Department of Optoelectronic Engineering, Jinan University, Guangzhou 510632, China; Cqd596918045@163.com (Q.C.); tzqchen@jnu.edu.cn (Z.C.)

* Correspondence: pxzhang@jnu.edu.cn (P.Z.); qhj@siom.ac.cn (H.Q.)

Abstract: β-Ga₂O₃ crystal have attracted great attentions in the fields of photonics and photoelectronics because of its ultra wide-band gap and high thermal conductivity. Here, pure β-Ga₂O₃ crystal was successfully grown by optical floating zone (OFZ) method, and used as saturable absorbers to realize a passively Q-switched all-solid-state 1μm laser for the first time. By placing the as-grown β-Ga₂O₃ crystal into the resonator of Nd:GYAP solid-state laser, a Q-switched pulses at the center wavelength of 1080.4 nm are generated under a output coupling of 10%. The maximum output power is 191.5 mW while the shortest pulse width is 606.54 ns, and the maximum repetition frequency is 344.06 kHz. The maximum pulse energy and peak power are 0.567 μJ and 0.93 W, respectively. Our experimental results show that β-Ga₂O₃ crystal has great potential in the development of all-solid-state 1μm pulsed laser.

Keywords: β-Ga₂O₃ crystal; optical floating zone; saturable absorber; Q-switch

1. Introduction

It is well known that saturable absorber plays an important role in Q-switching and mode locking operation[1-4]. Therefore, the development of different kinds of saturable absorbers as passive Q-switching devices to achieve high-quality pulsed laser output has always been a hot research field. At present, many studies on saturable absorbers are in

full swing, such as dyes, bulk semiconductors, two-dimensional materials and transition metal ion doped crystals[5-8]. The pulsed laser realized by some of the materials has made important application prospects in industrial processing, high-energy laser, scientific research and so on[9-11]. Especially in ~1μm near-infrared laser, which has the advantages of high pulse energy and high peak power, can be widely used in space communication, nonlinear spectroscopy, biomedicine, military and many other fields[12-14]. However, traditional materials often have their own shortcomings, such as limited types, single wavelength, and long-term operation stability to be improved. Therefore, how to develop a stable, reliable and efficient new saturable absorber for application in ~1μm near-infrared band is a problem worthy of further discussion.

Ga_2O_3 is a semiconductor material with ultra wide-band gap (~ 4.8ev), high conductivity [15-16]. Therefore, Ga_2O_3 is an electronic and optical material with great potential. Because of its unique physical and chemical properties, it has received great attention from researchers in different aspects, so it has been applied in many fields, including photo-detectors, photo-catalysis, field effect transistors and so on[17-20]. Ga_2O_3 is polymorphic, similar to Al_2O_3, is particularly interesting in applications, $β$-Ga_2O_3 has monoclinic structure and is the most stable phase, both physically and chemically[21-22]. $β$-Ga_2O_3 also inherits the excellent physical and chemical properties common to all phases of Ga_2O_3[23-24]. These excellent properties make us see that $β$-Ga_2O_3 has great potential for application in saturable absorbers. But as far as we know, there are still no reports on the application of pure $β$-Ga_2O_3 crystal to saturable absorbers, and even the application of other oxide materials to saturable absorbers is rarely reported.

In terms of $β$-Ga_2O_3 crystal growth method, the common large-size crystals growth method is melting method, including Czochralski method, EFG method, Bridgman method and so on[25-27]. We have successfully grown high-quality $β$-Ga_2O_3 by optical floating zone (OFZ) method. This method has the advantages of simple operation, low equipment requirements, and can grow even in the air environment. It solves many technical problems such as complex equipment, difficult operation, easy introduction of impurities, unable to guarantee the growth quality and so on[28-29]. We systematically characterized the chemical and optical properties of the synthesized $β$-Ga_2O_3. The crystal is of good quality which is pure and crack free. At the same time, we realized the optical modulation of the $β$-Ga_2O_3 in the pulse laser generation for the first time on the laser device with b-cut Nd:GYAP(Nd:$Gd_{0.1}Y_{0.9}AlO_3$) as the laser medium[30]. The maximum average output power is 195.1 mW which is obtained at 1080.4 nm. The corresponding shortest pulse duration is 606.54 ns and the maximum pulse repetition rate is 344.06 kHz. The maximum single pulse energy is 0.567 μJ and the maximum peak power is 0.93 W. From the experimental results, we have obtained a relatively stable pulsed laser with

short pulse width and large repetition frequency, which shows that the β-Ga_2O_3 has good saturable absorption properties. We believe that our work will provide an important reference for the potential applications of nonlinear optical devices related to crystal growth and optical modulation.

2. The preparation and characterization of the β-Ga_2O_3

The β-Ga_2O_3 single crystal was grown by the optical floating zone (OFZ) method using a Quantum Design IRF01-001-00 infrared image furnace. Ga_2O_3 powder (purity 99.9999 %) was employed as the raw material. The raw material was pressed into rod using a cold isostatic press. The rod was subsequently sintered at 1400°C for 10 h in air. And a <010> oriented crystal was used as the seed. Growth was carried out using Quantum Design IRF01-001-00 infrared image furnace. The sintered rod and seed were rotated at 10 rpm in opposite direction, and the crystal was grown in flowing air at the speed of 6 mm/h. Figure.1 shows the photo of as-grown β-Ga_2O_3 single crystal. After growth, as-grown sample was cutted into a size of 6 × 5 × 1 mm^3 wafer and subjected to chemical-mechanical-polishing into 0.5mm-thick wafer parallel to (100) plane to measure optical properties.
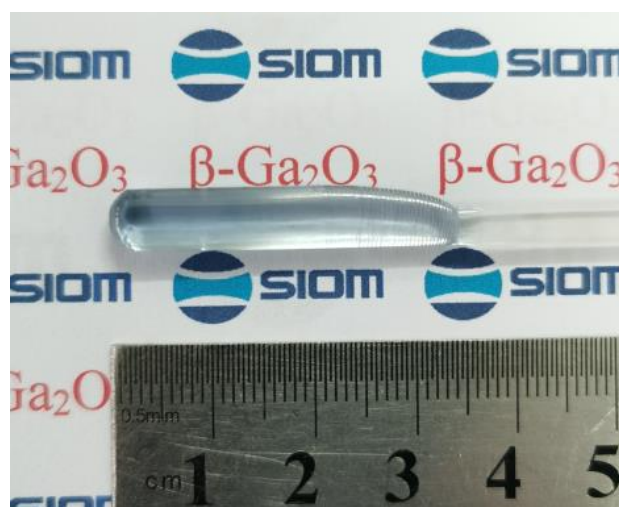

Figure. 1. The photo of as-grown β-Ga2O3 single crystal.

The X-ray rocking curve was measured using a Bruker D8 Discover X-ray diffractometer with a Cu Kα line at 40kV and 40mA. The optical transmittance spectrum was collected using a Lambda 1050+ UV/vis/NIR spectrometer (PerkinElmer). Figure.2 shows the X-ray rocking curve of the β-Ga_2O_3 (400) plane. The full-width at half-maximum (FWHM) is 100.8arcsec. It shows that the β-Ga_2O_3 crystal is the single crystal with good crystallization quality. Figure.3 shows the optical transmission spectrum of the β-Ga_2O_3 single crystal. β-Ga_2O_3 single crystal wafer indicates high transmittance between 80% and

82% from the visible wavelength to infrared (IR) wavelength region. The transmittance spectrum exhibits a cutoff absorption edge at around 255 nm. This was a result of the intrinsic absorption caused by the transition from the valence band to the conduction band[31].
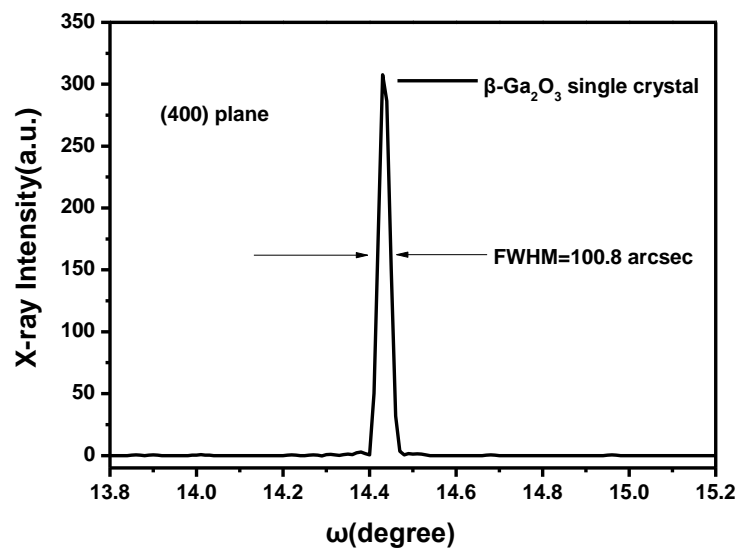

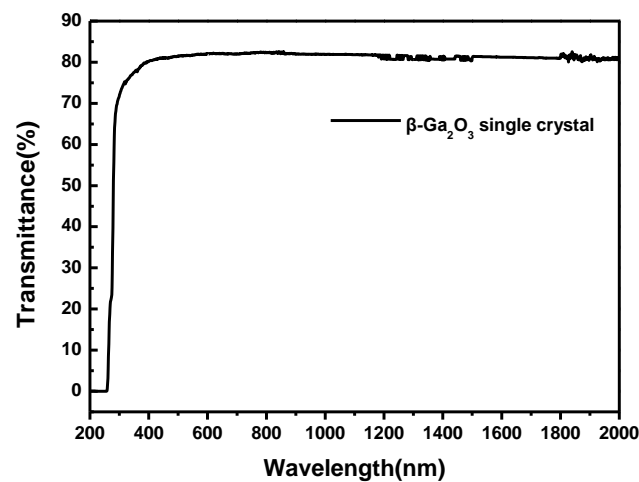**Figure. 2. X-ray rocking curve of the β-Ga₂O₃ single crystal [(400) plane].**

Figure. 3. X-ray rocking curve of the β-Ga₂O₃ single crystal [(400) plane].

3. Experimental results and discussion

In order to study the saturable absorption characteristics of β-Ga₂O₃ SA in the 1μm

wavelength region, a passively Q-switched laser composed of Nd:GYAP laser crystal and β-Ga_2O_3 SA was constructed as Figure. 4. The crystal was cut to 4 × 4 × 5 mm cuboid, along the b axis. The pump source is a 808 nm fiber-coupled semiconductor laser diode (LD), and the core diameter is 400 μm whose aperture is 0.22. Using an optical imaging system (1:1 imaging module), the spot radius of the pump laser beam focused on Nd:GYAP crystal is 200 μm. The resonator uses an input mirror M1 with high reflection from 1050 nm to 1100 nm and high transmittance from 800 nm to 820 nm, and an output mirror M2 with 10% transmittance from 1050 nm to 1100 nm. β-Ga_2O_3 SA is inserted between M2 and gain crystal. During normal operation, the Nd:GYAP crystal is wrapped in indium foil and maintained at 17 ° C by a chiller to minimize the thermal lens effect.
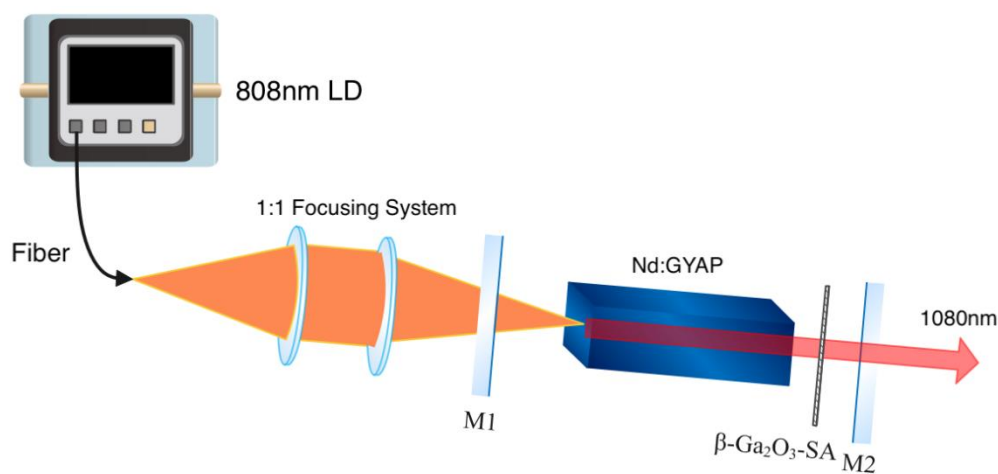
Figure. 4. Schematic experimental setup of the β-Ga_2O_3 SA Q-switched Nd:GYAP laser.

When no saturable absorber is added, a continuous wave (CW) with a threshold of 0.759 w is obtained. Then, we insert the prepared β-Ga_2O_3 SA into the laser cavity to realize Q-switched pulse. During the experiment, the average output power of CW and Q-switched lasers is measured as a function of pump power. It is obvious from Figure. 5 that the average output power of the two groups increases linearly with the pump power. After linear fitting, the slope efficiency of CW and Q-switched lasers are 28.6% and 10.2% respectively. When the absorption pump power of CW laser is 3.75 W, the maximum output power is 0.9262 W, and at this time, it reaches the highest Q-switched average output power of 195.1 mW. The slope efficiency of Q-switched laser is lower than that of continuous laser, which is mainly due to the unsaturated absorption loss of Ga_2O_3 SA.
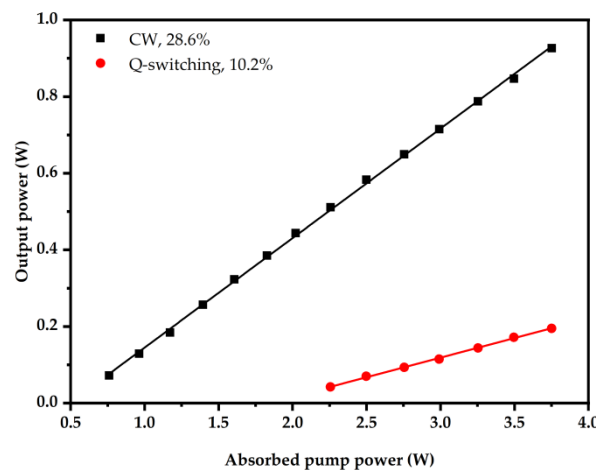
Figure. 5. The average output power of Nd: GYAP laser in different operation regimes.

The pulse generation is due to the sudden decrease of laser oscillation threshold caused by the complete saturated absorption of SA. After the first pulse output, the absorption of SA returns to a higher initial value, and the inverted particle swarm can accumulate again to prepare for the formation of the next pulse. According to the principle of passive Q-switched, at high pump power, short saturation absorption period and strong stimulated radiation are helpful to produce pulses with high repetition rate and narrow pulse width respectively. Therefore, with the increase of pump power, the duration of Q-switched pulse narrows, and the number of pulses in the same time period increases. Figure.6 shows the variation of pulse width and repetition frequency with pump power. With the increase of pump power from 2.256 W to 3.751 W, the repetition rate curve shows a continuous upward trend from 88.67 kHz to 344.06 kHz while the width of a single pulse decreases from 2030.39 ns to 606.54 ns. Figure.7 shows the oscilloscope image at the highest repetition frequency and the shortest pulse. Through the relatively neat pulse sequence in the picture, we can also know that we have obtained a relatively stable and neat pulse laser.
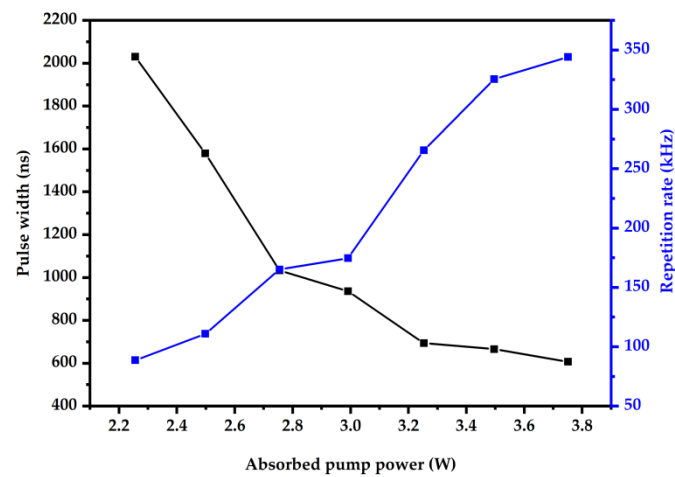
Figure. 6. Dependences of pulse width and repetition rate on absorbed pump power.
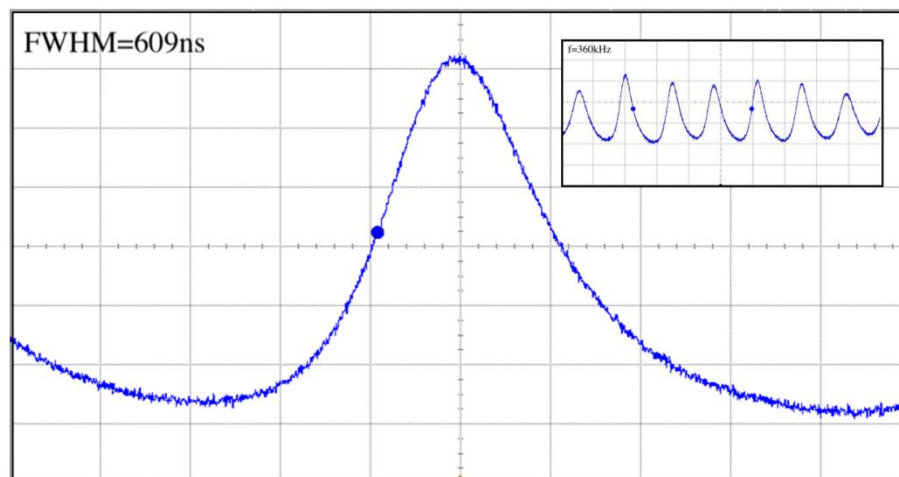

Figure. 7. Temporal pulse train and single pulse profile from the β-Ga₂O₃-SA Q-switched Nd: GYAP laser.

Based on the average output power, pulse width and repetition frequency, the corresponding single pulse energy and peak power of Q-switched laser are calculated. The single pulse energy and peak power increase with the increase of pump power, which proves that our laser output is Q-switched mode rather than relaxation oscillation mode. When the pump power is 3.75 W, the maximum single pulse energy is 0.567 μJ. The maximum peak power is 0.93 W. We also measured the central wavelength of laser emission. Figure. 8 shows the emission wavelength in the Q-switched region, with a peak at about 1080.4 nm. The inserted β-Ga₂O₃ SA does not change the emission wavelength of

Nd:GYAP laser.

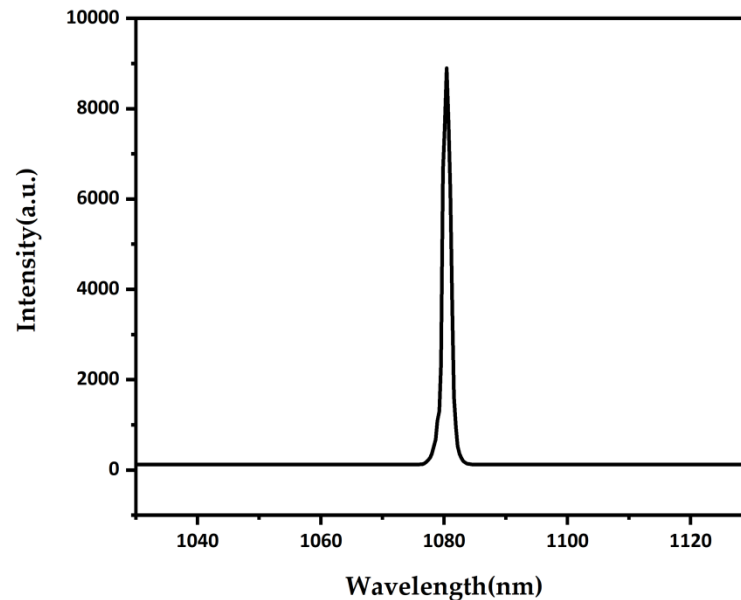**Figure. 8. The laser emission spectrum of Nd: GYAP laser in Q-switching regimes.**

4.Conclusion

In summary, we have successfully grown high-quality β-Ga$_2$O$_3$ by OFZ method, and firstly used them as saturable absorbers to realize the output of pulsed laser. The synthetic method is simple and practical, with low cost and low environmental requirements, and the grown crystal is pure and crack free. At the same time, the β-Ga$_2$O$_3$ crystal is applied to Nd:GYAP solid-state laser for the first time, and the pulsed laser output is realized. The maximum average output power of 195.1 mW is obtained at 1080.4 nm. The corresponding minimum pulse width is 606.54 ns and the maximum pulse repetition frequency is 344.06 kHz. Our results will promote the research of more Q-switched crystals and expand their potential applications in the field of ultra-fast photonics.

Acknowledgements

Reference

1 Namour, M.; Mobadder, M.; Magnin, D.; Peremans, A.; Verspecht, T.; Teughels, W.; Lamard, L.; Nammour, S.; Rompen, E. Q-Switch Nd:YAG laser-assisted decontamination of implant surface. *Dent J (Basel)*. **2019**, 7, 99. doi:10.3390/dj7040099.

2 Namour, M.; Verspecht, T.; Mobadder, M.; Teughels, W.; Peremans, A.; Nammour, S.; Rompen, E. Q-Switch Nd:YAG laser-assisted elimination of multi-species biofilm on titanium surfaces. *Materials (Basel)*. **2020**, 13, 1573. doi:10.3390/ma13071573.

3 Cong, Z.; Liu, Z.; Qin, Z.; Zhang, X.; Wang, S.; Rao, H.; Fu, Q. RTP Q-switched single-longitudinal-mode Nd:YAG laser with a twisted-mode cavity. *Appl Opt*. **2015** 54(16):5143-5146. doi: 10.1364/AO.54.005143.

4 Suzuki, M.; Boyraz, O.; Asghari, H.; Jalali, B. Spectral dynamics on saturable absorber in mode-locking with time stretch spectroscopy. *Sci Rep*. **2020**, 10(1):14460. doi: 10.1038/s41598-020-71342-x.

5 Ren, C.; Deng, X.; Hu, W.; Li, J.; Miao, X.; Xiao, S.; Liu, H.; Fan, Q.; Wang, K.; He, T. A near-infrared I emissive dye: toward the application of saturable absorber and multiphoton fluorescence microscopy at the deep-tissue imaging window. *Chem Commun (Camb)*. **2019**, 25, 35: 5111-5114. doi: 10.1039/c9cc02120e.

6 Wang, M.; Zheng, Y.; Guo, L.; Chen, X.; Zhang, H.; Li, D. Nonlinear optical properties of zirconium diselenide and its ultra-fast modulator application. *Nanomaterials (Basel)*. **2019**, 9: 1419. doi: 10.3390/nano9101419.

7 Yang, J.; Tian, K.; Li, Y.; Dou, X.; Ma, Y.; Han, W.; Xu, H.; Liu, J. Few-layer Bi_2Te_3: an effective 2D saturable absorber for passive Q-switching of compact solid-state lasers in the 1-μm region. *Opt Express*. **2018**, 26(17):21379-21389. doi: 10.1364/OE.26.021379.

8 Ge, W.; Zhang, H.; Wang, J.; Cheng, X.; Jiang, M.; Du, C.; Yuan, S. Pulsed laser output of LD-end-pumped 1.34 mum Nd:GdVO$_4$ laser with Co:LaMgAl$_{11}$O$_{19}$ crystal as saturable absorber. *Opt Express*. **2005**, 13(10):3883-3889. doi: 10.1364/opex.13.003883.

9 Malinauskas, M.; Žukauskas, A.; Hasegawa, S.; Hayasaki, Y.; Mizeikis, V.; Buividas, R.; Juodkazis, S. Ultrafast laser processing of materials: from science to industry. *Light Sci Appl*. **2016**, 5: e16133. doi: 10.1038/lsa.2016.133.

10 Kouno, A.; Watanabe, S.; Hongo, T.; Yao, K.; Satake, K.; Okiji, T. Effect of pulse energy, pulse frequency, and tip diameter on intracanal vaporized bubble kinetics and apical pressure during laser-activated irrigation using Er:YAG Laser. *Photomed Laser Surg*. **2020**, 38(7):431-437. doi: 10.1089/photob.2019.4739.

11 Ge, Z.; Saito, T.; Kurose, M.; Kanda, H.; Arakawa, K.; Takeda, M. Precision

interferometry for measuring wavefronts of multi-wavelength optical pickups. *Opt Express*. **2008**, 7, 16(1):133-143. doi: 10.1364/oe.16.000133.

12 Griffith, R.; Simmons, B.; Bray, F.; Falto-Aizpurua, L.; Abyaneh, M.; Nouri, K. 1064 nm Q-switched Nd:YAG laser for the treatment of Argyria: a systematic review. *J Eur Acad Dermatol Venereol*. **2015**, 29(11): 2100-2103. doi: 10.1111/jdv.13117.

13 Chang, Y.; Lee, J.; Jhon, Y.; Lee, J. Active Q-switching in an erbium-doped fiber laser using an ultrafast silicon-based variable optical attenuator. *Opt Express*. **2011**, 19(27):26911-26916. doi: 10.1364/OE.19.026911.

14 Cabalín, L.; González, A.; Lazic, V.; Laserna, J. Deep ablation and depth profiling by laser-induced breakdown spectroscopy (LIBS) employing multi-pulse laser excitation: application to galvanized steel. *Appl Spectrosc*. **2011**, 65(7): 797-805. doi: 10.1366/11-06242.

15 Kim, S.; Lee, H.; Oh, S.; Noh, B.; Park, S.; Im, Y.; Son, S.; Song, Y.; Kim, K. Transparent conductive electrodes of β-Ga_2O_3/Ag/β-Ga_2O_3 multilayer for ultraviolet emitters. *J Nanosci Nanotechnol*. **2019**, 19(10): 6328-6333. doi: 10.1166/jnn.2019.17053.

16 An, Y.; Shen, X.; Hao, Y.; Guo, P.; Tang, W. Enhanced resistance switching of Ga_2O_3 thin films by ultraviolet radiation. *J Nanosci Nanotechnol*. **2020**, 20(5): 3283-3286. doi: 10.1166/jnn.2020.17426.

17 Ma, J.; Yoo, G. Electrical properties of top-gate β-Ga_2O_3 nanomembrane metal-semiconductor field-effect transistor. *J Nanosci Nanotechnol*. **2020**, 20(1): 516-519. doi: 10.1166/jnn.2020.17259.

18 Bae, H.; Yoo, T.; Yoon, Y.; Lee, I.; Kim, J.; Cho, B.; Hwang, W.; High-aspect ratio β-Ga_2O_3 nanorods via hydrothermal synthesis. *Nanomaterials (Basel)*. **2018**, 8(8):594. doi: 10.3390/nano8080594.

19 Long, X.; Niu, W.; Wan, L.; Chen, X.; Cui, H.; Sai, Q.; Xia, C.; Devki N. Talwar.; Feng, Z.; Optical and Electronic Energy Band Properties of Nb-Doped β-Ga_2O_3 crystals. *Crystals*. **2021**, 11, 135. doi.org/10.3390/cryst11020135.

20 Hisatomi, T.; Brillet, J.; Cornuz, M.; Le Formal, F.; Tétreault, N.; Sivula, K.; Grätzel, M. A Ga_2O_3 underlayer as an isomorphic template for ultrathin hematite films toward efficient photoelectrochemical water splitting. *Faraday Discuss*. **2012**, 155:223-232. doi: 10.1039/c1fd00103e.

21 Zhou, H.; Zeng, S.; Zhang, J.; Liu, Z.; Feng, Q.; Xu, S.; Zhang, J.; and Hao, Y. Comprehensive Study and Optimization of Implementing p-NiO in β-Ga_2O_3 Based Diodes via TCAD Simulation. *Crystals*. **2021**, 11, 1186. doi.org/10.3390/cryst11101186.

22 Reddy, L.; Ko, Y.; Yu, J.; Hydrothermal synthesis and photocatalytic property of β-Ga_2O_3 nanorods. *Nanoscale Res Lett*. **2015**, (10): 364. doi: 10.1186/s11671-015-1070-5.

23 Huan, Y.; Sun, S.; Gu, C.; Liu, W.; Ding, S.; Yu, H.; Xia, C.; Zhang, D.; Recent advances in β-Ga$_2$O$_3$-Metal contacts. *Nanoscale Res Lett*. **2018**, 13(1): 246. doi: 10.1186/s11671-018-2667-2.

24 Cui, W.; Ren, Q.; Zhi, Y.; Zhao, X.; Wu, Z.; Li, P.; Tang, W. Optimization of growth temperature of β-Ga$_2$O$_3$ thin films for solar-blind photodetectors. *J Nanosci Nanotechnol*. **2018**, 18(5):3613-3618. doi: 10.1166/jnn.2018.14692.

25 Yeom, T.; Lim, A.; Study of nuclear quadrupole interactions and quadrupole Raman processes of ^{69}Ga and ^{71}Ga in a β-Ga$_2$O$_3$:Cr^{3+} single crystal. *J Magn Reson*. **2009** , 200(2):261-266. doi: 10.1016/j.jmr.2009.07.008.

26 Xue, H.; He, Q.; Jian, G.; Long, S.; Pang, T.; Liu, M. An overview of the ultrawide bandgap Ga$_2$O$_3$ Semiconductor-Based schottky barrier diode for power electronics application. *Nanoscale Res Lett*. **2018**, 13(1):290. doi: 10.1186/s11671-018-2712-1.

27 Hoshikawa, K.; Kobayashi, T.; Ohba, E.; Kobayashi, T.; 50mm diameter Sn-doped (001) β-Ga$_2$O$_3$ crystal growth using the Vertical Bridegman Technique in ambient air. *J Cryst Growth*. **2020**, 546, 125778. doi.org/10.1016/j.jcrysgro.2020.125778.

28 Abbene, L.; Principato, F.; Gerardi, G.; Buttacavoli, A.; Cascio, D.; Bettelli, M.; Amadè, N.; Seller, P.; Veale, M.; Fox, O.; Sawhney, K.; Zanettini, S.; Tomarchio, E.; Zappettini, A. Room-temperature X-ray response of cadmium-zinc-telluride pixel detectors grown by the vertical Bridgman technique. *J Synchrotron Radiat*. **2020**, 27(Pt 2):319-328. doi: 10.1107/S1600577519015996.

29 Kozhemyakin, G.; Nemets, L.; Bulankina, A. Simulation of ultrasound influence on melt convection for the growth of Ga$_x$In$_{1-x}$Sb and Si single crystals by the Czochralski method. *Ultrasonics*. **2014**, 54:2165-2168. doi: 10.1016/j.ultras.2014.06.006.

30 Zhou, H.; Zhu, S.; Li, Z.; Yin, H.; Zhang, P.; Chen, Z.; Fu, S.; Zhang, Q.; Lv, Q. Investigation on 1.0 and 1.3 μm laser performance of Nd^{3+}: GYAP crystal. *Opt. Laser Technol*. **2019**, 119, 105601. doi: org/10.1016/j.optlastec.2019.105601.

31 Li, P.; Bu, Y.; Chen, D.; Sai, Q.; and Qi, H. Investigation of the crack extending downward along the seed of the β-Ga$_2$O$_3$ crystal grown by the EFG method. *CrystEngComm*, **2021**, 23:6300-6306. doi: 10.1039/d1ce00576f